Ab Initio Tests of the Marcus Equation for the Prediction of the Position of the Transition State for the Reaction $H + C_2H_5R \rightarrow CH_4 + CH_2R$ with R = H, CH_3, NH_2, CN, CF_3, and C_6H_5

W. T. Lee and Richard I. Masel*

Department of Chemical Engineering, University of Illinois at Urbana−Champaign, Urbana, Illinois 61801-3792

Received: June 13, 1997; In Final Form: August 1, 1997

Marcus originally derived the Marcus equation to predict Brønsted coefficients for electron-transfer reactions. However in the literature it is often assumed that Marcus' result can be extended to predict positions of the transition state for atom-transfer reactions. In this paper we use ab initio methods to examine the potential energy surface and transition state of a series of hydrogenolysis reactions of the form $H^{\bullet} + CH_3CH_2R \rightarrow CH_4 + {}^{\bullet}CH_2R$, with R = H, CH_3, CF_3, CN, NH_2, and C_5H_6, in order to see if the Marcus equation can be extended to atom-transfer reactions. The calculations show that the molecular orbitals of the system look "reactant-like" moving up the potential energy surface toward the transition state, and then switch to "product-like" moving down to products, in qualitative agreement with what one would expect from the Marcus equation. However, the curve crossing from "reactant-like" to "product-like" molecular orbitals does not occur at the saddle point in the potential energy surface. Rather the curve crossing occurs at a point part way down to products. Also most of the barrier to reaction is associated with rearrangements of the electron clouds due to Pauli repulsions when the reactants come together and not with the bond destruction and bond formation processes. These rearrangements are not considered in the Marcus equation. We do not yet know if our results are special to the reactions here or are general. However, it does appear that some key physics is missing when one extends the Marcus model to atom- or ligand-transfer reactions. One can represent the key physics with a modified bond additivity potential, however.

Introduction

In 1969, Polayni and Wong[25] were examining the properties of H_2/F_2 chemical lasers. They pointed out that in order for a chemical reaction to produce vibrationally excited species which could lase, the reaction must have an early transition state. Soon, several investigators were proposing models to relate the transition-state position to molecular properties. A few years before, Marcus[1] had examined the Brønsted coefficient, γ_P, for electron-transfer reactions. As part of the derivation Marcus also obtained an expression for $\chi^{\ddagger}$, the position of the transition state during the reaction:

$$\chi^{\ddagger}(\text{Marcus}) = 0.5 + \frac{\Delta H}{8E_a^{\circ}} \qquad (1)$$

where $\chi^{\ddagger}$ is the position of the transition state in dimensionless coordinates, ΔH is the heat of reaction, and E_a° is the intrinsic activation barrier. Marcus suggested that eq 1 was useful for electron-transfer reactions but *not* atom- or ligand-transfer reactions.[2] Nevertheless after people became interested in the position of the transition state, Murdoch,[21] Sutin,[22] and Albey[23] asserted that eq 1 could also be used to predict the position of the transition state for atom- and ligand-transfer reactions in chemical lasers.

Their analysis was based on the curve-crossing model in Figure 1. The system goes up the reactant potential, crosses at the curve crossing, and then goes down the product potential.

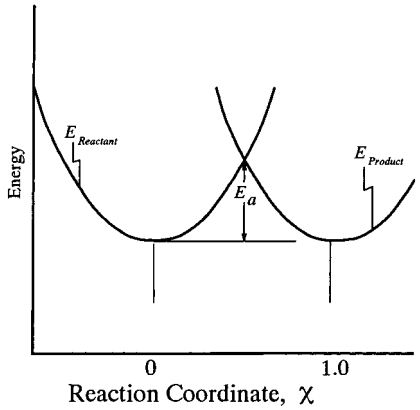

Figure 1. Change in the energy of the system as the reaction proceeds, after Murdoch[21] and Marcus.[22]

So far very little work has been done to critically test the extension of the Marcus Brønsted formulation to the prediction of the position state in ligand-transfer reactions. Lee and Masel,[3] Yamataka et al.,[4] and Shaik and Schlegel[5] have used eq 1 to estimate Brønsted coefficients in atom-transfer reactions. However, little work has been done to see if the formulation can predict the position of the transition state for atom- or ligand-transfer reactions.

In this paper we will use ab initio calculations to estimate $\chi^{\ddagger}$ at the transition state and compare to eq 1.

Background

First we need a suitable definition to quantify χ. At this point it is unclear what value of $\chi^{\ddagger}$ is being measured experimentally.

* To whom correspondence should be addressed.

S1089-5639(97)01955-5 CCC: $15.00
Published on Web 03/06/1998

Pross and Shaik[6] suggest that in principle many different reaction parameters such as the extent of bond-forming, bond-breaking, charge transfer, solvation, and others can each be used to define the reaction coordinate, and one can use the definition of χ to define a value of $\chi^{\ddagger}$. The only desired constraint that Pross and Shaik impose is that χ be 0 at the position of reactants, 1.0 at the position of the products, and vary smoothly in between. Still, in practice most investigators use the extent of bond-forming and bond-breaking to define a numeral value at χ. For example if one adopts Pauling's[7] definition of bond order,

$$n = \exp(-(r - r_{eq})/a) \tag{2}$$

where r_{eq} is the equilibrium bond length of the bond and a is a scaling constant, one can define a reaction coordinate via

$$\chi(\text{Pauling}) = \frac{n_f}{n_f + n_b} \tag{3}$$

where n_f is the bond order of the forming bond, while n_b is the bond order of the breaking bond at the position of the transition state. Equation 3 is the definition of the position of the transition state used most often in the literature. Marcus (personal communication, 1996, 1997) suggests that this definition is appropriate for his model.

One can also easily define a satisfactory definition of χ based on the atomic coordinates:

$$\chi(\text{Geom}) = \frac{(r^* - r_{eq})_b}{(r^* - r_{eq})_b + (r^* - r_{eq})_f} \tag{4}$$

where subscript b and f denote the breaking and the forming bonds, respectively. Although other properties of transition state (such as the extent of bond bending, the amount of electronic population in certain orbitals, the extent of orbital overlap) can also be used in the definition of reaction coordinate, none of them have been used extensively in the context of reaction coordinate.

We also need to note that alternatives to the Marcus equation have been suggested in the literature. In 1955, Hammond[8] proposed a simple qualitative postulate to relate the position of the transition state to the energetics of the reaction. Hammond's ideas were based on earlier work of Brønsted[9] and Leffler.[10] According to Hammond's postulate, $\chi^{\ddagger}$ is given by

$$\chi^{\ddagger} = \frac{(E_a - E_a^{\circ})}{\Delta H} \tag{5}$$

where E_a is the activation barrier to the reaction, E_a° is the intrinsic activation energy, and ΔH is the heat of reaction. In the electrochemical literature, Bockris[11] has shown that one can determine the value of $\chi^{\ddagger}$ from

$$\chi^{\ddagger}(\text{Bockris}) = \frac{S_r}{(S_r + S_p)} \tag{6}$$

where S_r and S_p are the average slopes of the intrinsic reaction coordinate (IRC) curve on the reactant side and on the product side, respectively.

From purely mathematical considerations, Miller[12] and Agmon[13] have independently shown that, assuming certain general properties of the potential energy profile, the position of transition state can be given by

$$\chi^{\ddagger}(\text{Miller}) = \frac{1}{2 - (\Delta H/E_a)} \tag{7}$$

Still, eqs 6, 7, and 8 were derived using formulations similar to those of Marcus. One does not know a priori whether these formulations are correct.

In the previous literature, there have only been a few attempts to use ab initio calculations to test eqs 1 and 6−8. Several years ago, Yamataka[4] et al. did Hartree−Fock calculations and found little agreement between $\chi^{\ddagger}$ calculated from the transition-state geometry and that calculated from eq 1. More recently Lee and Masel[3] used high-level calculations to test eqs 1, 6, and 7 for an atom-transfer reaction and found reasonable agreement between $\chi^{\ddagger}$ estimated from ab initio calculations and that from Bockris' result (eq 6) but little agreement with $\chi^{\ddagger}$ estimated from the Marcus equation, eq 1, or Miller's result, eq 7. In particular, Lee and Masel were examining cases with late or very late transition states, but the Marcus equation and Miller's results predicted early transition states for these cases. Lee and Masel suggested that the differences arose because the Pauli repulsions, which are ignored in the derivation of the Marcus equation, played a key role in determining the position of the transition state.

In this paper, we will do calculations to see if the Marcus equation can be used to predict the position of the transition state for ligand-transfer reactions. We consider the series of reactions

$$H + C_2H_5R \rightarrow CH_4 + CH_2R \tag{8}$$

with R = H, CH_3, NH_2, CN, CF_3, and C_6H_5. This set of reactions was chosen because our previous work has shown that the Pauli repulsions are particularly strong in the reaction

$$D + C_2H_6 \rightarrow DCH_3 + CH_3 \tag{9}$$

Therefore, one might think that the reactions in eq 9 would show interesting deviations from the Marcus result. In this paper, ab initio calculations have been used to see if the Marcus formulation applies to this system. We also test Murdoch's idea that we can represent the transition state as a curve crossing between two parabolic potential energy manifolds.

Calculational Methods

Ab initio MO calculations were carried out for all the molecules and transition states. Geometries of equilibrium molecules were fully optimized at the second-order Moller−Plesset perturbation theory (MP2) using a 6-31G(d) basis set with d-polarization function added to the heavy atoms. To optimize the geometry of the transition states, polarization functions (p-type) were also added to the hydrogen atoms due to the large C−H bond distance at the transition state. In all the calculations, spin projection[14] was used to correct for spin contamination in open shell structures. Frequency calculations were performed to check for the imaginary frequencies of the transition states.

Single-point calculations at fourth-order Moller−Plesset perturbation theory (MP4SDTQ) and quadratic configuration interaction (QCISD(T)) were then carried out to determine the energetics of the molecules and transition states, except for R = C_6H_5. These high-level calculations were done using the 6-311G(d,p) basis set. We also did calculations using the G-2 theory,[15] where the zero-point energies and other high-level corrections were included in the calculations. Due to the large

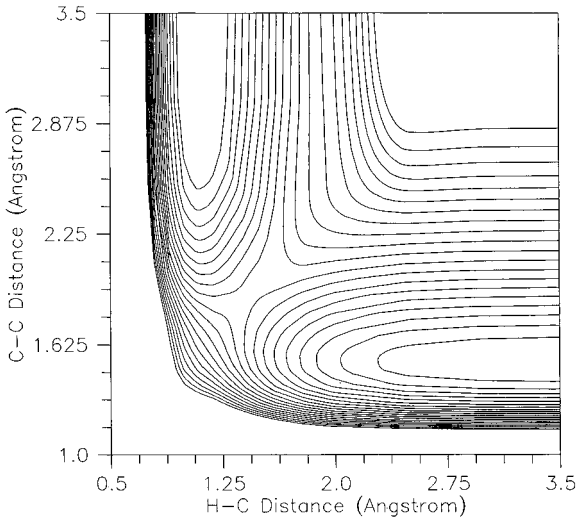

Figure 2. Potential energy surface for the reaction $H + C_2H_6 \rightarrow CH_4 + CH_3$ calculated at the MP2/6-31G(d,p) level.

calculations for $R = C_6H_5$, the energetics were determined at the PMP2/6-31+G(d,p) level.

To determine the slopes of the potential energy profiles as mentioned in eq 2, intrinsic reaction coordinate (IRC) calculations[16] were carried out to trace the mass-weighted reaction path leading down from the transition state toward the reactants and products. This was done using a 6-31+G(d,p) basis set. The slopes at the inflection points of the energy were then used in eq 2.

We used two different approximations to calculate the intrinsic activation energies. The first is based on the Hammond postulate

$$E^{\circ}_{AB} = E_{AB} - \chi^{\ddagger}\,\Delta H \tag{10}$$

The second is based on Marcus' additivity postulate

$$E^{\circ}_{AB} = \frac{1}{2}(E^{\circ}_{AA} + E^{\circ}_{BB}) \tag{11}$$

where E°_{AA} and E°_{BB} are the activation barriers for the corresponding symmetric bond scissions. In the cases considered here eqs 10 and 11 gave the same result to within 1 kcal/mol.

All of the calculations in this paper were done with the GAUSSIAN92[17] and GAUSSIAN94[18] programs.

Results

Figure 2 shows a potential energy surface for the reaction $H + C_2H_6 \rightarrow CH_4 + CH_3$. In the calculation the hydrogen radical was assumed to approach the CH_3CH_2R molecule along the C−C axis. We have also looked at cases where the radical attacks perpendicular to the C−C bond or at other angles, but found that the activation barrier is higher along these other pathways.

Figure 2 looks standard for a S_N2 reaction. There is a small van der Waals attraction on the reactant side of the molecule and a fairly symmetric barrier.

Figure 3 shows the geometries of the transition-state structures calculated at PMP2/6-31G(d,p) level of theory. Table 1 lists the bond lengths of the forming and the breaking bonds at the transition states, along with their corresponding equilibrium bond lengths in the reactants and products. We have also included the structures optimized using other basis sets wherever possible for comparison. It is found that in general, with a larger basis set, the optimized bond lengths are shorter. The p-polarization function added to the hydrogen appears to be essential when doing geometry optimization of the transition states. The optimized structures compare favorably to the available experimental values obtained from the CRC Handbook,[19] as shown in Table 2.

The energetics of the reactions calculated at the MP4(SDTQ) and QCISD(T) level are summarized in Table 3. It is found that a higher level of calculation results in more exothermic

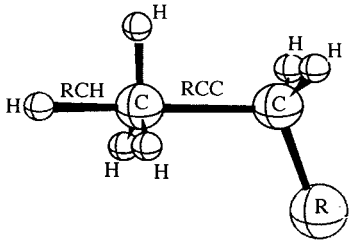

Figure 3. Geometries of the transition state found in the calculations reported in this paper.

TABLE 1: Comparison of the Equilibrium Bond Lengths with the Bond Lengths at the Transition State

		transition state		equilibrium	
R group	method/basis sets	r_{CH}	r_{CC}	r_{CH}	r_{CC}
H	UMP2/6-31G	1.383	1.875	1.095	1.545
	UMP2/6-31G(d)	1.383	1.875	1.090	1.526
	UMP2/631-G(d,p)	1.369	1.853	1.085	1.523
	UMP2=(FULL)/6-31G(d,p)	1.368	1.852	1.090	1.524
	UMP2/6-31+G(d,p)	1.367	1.851	1.086	1.525
	UMP2/6-311G(d)	1.375	1.871	1.089	1.528
	UMP2/6-311G(d,p)	1.364	1.855	1.090	1.529
	UMP2/6-311+G(d,p)	1.364	1.852	1.090	1.529
	UMP2/6-311++G(d,p)	1.363	1.852	1.090	1.529
CH_3	UMP2/6-31G	1.448	1.915	1.095	1.545
	UMP2/6-31G(d,p)	1.373	1.847	1.085	1.524
	UMP2=(FULL)/6-31G(d,p)	1.372	1.846	1.090	1.525
	UMP2/6-31+G(d,p)	1.372	1.845	1.086	1.525
	UMP2/6-311G(d,p)	1.367	1.848	1.090	1.528
NH_2	UMP2/6-31G	1.489	1.929	1.095	1.510
	UMP2=(FULL)/6-31G(d,p)	1.402	1.849	1.090	1.526
	UMP2/6-31+G(d,p)	1.400	1.844	1.086	1.490
CN	UMP2/6-31G	1.377	1.897	1.095	1.552
	UMP2=(FULL)6-31G(d,p)	1.349	1.838	1.090	1.530
	UMP2/6-31+G(d,p)	1.348	1.837	1.086	1.531
CF_3	UMP2/6-31G	1.430	1.910	1.095	1.544
	UMP2=(FULL)/6-31G(d,p)	1.363	1.845	1.090	1.523
	UMP2/6-31+G(d,p)	1.365	1.851	1.086	1.525
C_6H_5	UMP2/6-31+G(d,p)	1.368	1.832	1.086	1.53

TABLE 2: Geometries of Selected Molecules, Selected at UMP_2=(FULL)/6-31G(d), Compared with Established Experimental Values from the CRC Handbook

molecule	structures	optimized value	exptl values
CH_3	R_{CH}	1.078	1.08
CH_4	R_{CH}	1.090	1.0870
C_2H_6	R_{CC}	1.524	1.5351
	R_{CH}	1.093	1.0940
	$\angle_{CCH}$	111.2	111.17
C_3H_8	R_{CC}	1.525	1.532
	R_{CH}	1.096	1.107
	$\angle_{CCC}$	112.4	112
$C_2H_5NH_2$	R_{CN}	1.464	1.471[a]
	R_{NH}	1.019	1.010[a]
C_2H_5CN	R_{CN}	1.179	1.159[b]
$C_2H_5CF_3$	R_{CF}	1.353	1.332[c]
$C_2H_5(C_6H_5)$	R_{CC}(aromatic)	1.398	1.399[d]

[a] Values from methylamine, CH_3NH_2. [b] Values from acetonitrile, CH_3CN. [c] Values from fluoroform, CHF_3. [d] Values from benzene, (C_6H_5).

TABLE 3: Total Energies of the System Calculated at Various Levels of Theory

		energies (hartrees)						
R group	level of calculation	H	C_2H5_R	H--CH_3--CH_2R	CH_4	CH_2R	E_a (kcal/mol)	ΔH (kcal/mol)
H	PMP2/6-31G+(d,p)	−0.499 81	−79.570 89	−80.007 25	−40.379 23	−39.709 17	39.81	−11.11
	UMP4(SDTA)/6-31G+(d,p)	−0.499 81	−79.614 52	−80.047 94	−40.405 03	−39.730 77	41.66	−13.47
	QCISD(T)/6-31G+(d,p)	−0.499 81	−79.615 79	−80.052 58	−40.405 89	−39.732 24	39.55	−14.14
	G2 theory	−0.500 00	−79.630 86	−80.071 31	−40.410 88	−39.745 09	37.37	−15.76
CH_3	PMP2/6-31G+(d,p)	−0.499 81	−118.766 05	−119.204 40	−40.379 23	−78.905 07	38.56	−11.57
	UMP4(SDTQ)/6-31G+(d,p)	−0.499 81	−118.827 27	−119.262 63	−40.405 03	−78.944 59	40.44	−14.14
	QCISD(T)/6-31G+(d,p)	−0.499 81	−118.828 79	−119.267 43	−40.405 89	−78.946 63	38.39	−15.01
	G2 theory	0.500 00	−118.855 80	−119.300 72	−40.410 88	−78.969 25	34.56	−15.27
NH_2	PMP2/6-31G+(d,p)	−0.499 81	−134.786 17	−135.288 48	−40.379 23	−94.935 76	36.08	−18.20
	UMP4(SDTQ)/6-31G+(d,p)	−0.499 81	−134.841 86	−135.281 20	−40.405 03	−94.969 35	37.95	−20.52
	QCISD(T)/6-31G+(d,p)	−0.499 81	−134.842 89	−135.285 76	−40.405 89	−94.971 26	35.73	−21.62
	G2 theory	−0.500 00	−134.894 57	−135.340 47	−40.410 88	−95.018 58	33.95	−21.89
CN	PMP2/6-31G+(d,p)	−0.499 81	−171.601 75	−172.043 05	−40.379 23	−131.746 10	36.71	−14.92
	UMP4(SDTQ)/6-31G+(d,p)	−0.499 81	−171.660 86	−172.097 37	−40.405 03	−131.777 87	39.72	−13.95
	QCISD(T)/6-31G+(d,p)	−0.499 81	−171.657 59	−172.099 87	−40.405 89	−131.783 18	36.10	−19.88
	G2 theory	−0.500 00	−171.747 62	−172.193 98	−40.410 88	−131.869 46	33.66	−20.53
CF_3	PMP2/6-31G+(d,p)	−0.499 81	−416.017 15	−416.454 79	−40.379 23	−376.148 52	39.01	−6.77
	UMP4(SDTQ)/6-31G+(d,p)	−0.499 81	−416.084 50	−416.519 33	−40.405 03	−376.193 90	40.78	−9.18
	QCISD(T)/6-31G+(d,p)	−0.499 81	−416.081 22	−416.519 16	−40.405 89	−376.191 29	38.83	−10.14
	G2 theory	−0.500 00	−416.358 89		−40.410 88	−376.464 98		−10.65
C_6H_5	PMP2	−0.498 23	−309.891 99	−310.324 86	−40.365 95	−270.059 02	41.01	−21.81

heats of reactions and lower activation energies. This is mainly due to the fact that the inclusion of a higher level of correlation energies stabilizes the transition state and the product radicals more than the reactants.

Figure 4 shows the results of the IRC calculations. In an IRC calculation, the transition state is arbitrarily set to zero on the reaction coordinate and the reaction coordinate is normalized so that the reactants are toward the negative direction while the products are toward the positive direction. The slopes of the potential energy curves were determined and the values were used in eq 2 to calculate the positions of the transition state.

A summary of the positions of the transition state calculated from various equations described earlier is provided in Table 4. The ab initio calculations show that the reactions considered here all have late transition states ($\chi^{\ddagger} \sim 0.5-0.54$); however, the Marcus equation and Miller's equation predict an early transition state ($\chi^{\ddagger} \sim 0.39-0.46$). Bokris's method predicts $\chi^{\ddagger}$ of 0.55−0.59, i.e., later transition states than the ab initio calculations.

Figure 5 shows the actual transition-state position as a function of $\Delta H/E_a^{\circ}$. The lines are the prediction of eqs 1, 7, 21, and 11, while the points are the ab initio calculations. We included both the forward and reverse reactions to get a consistent picture. Generally, there is little correlation between the Marcus equation and Miller's equation and the ab initio results. Equations 21 and 22, which we will discuss later in the paper, fit much better, however.

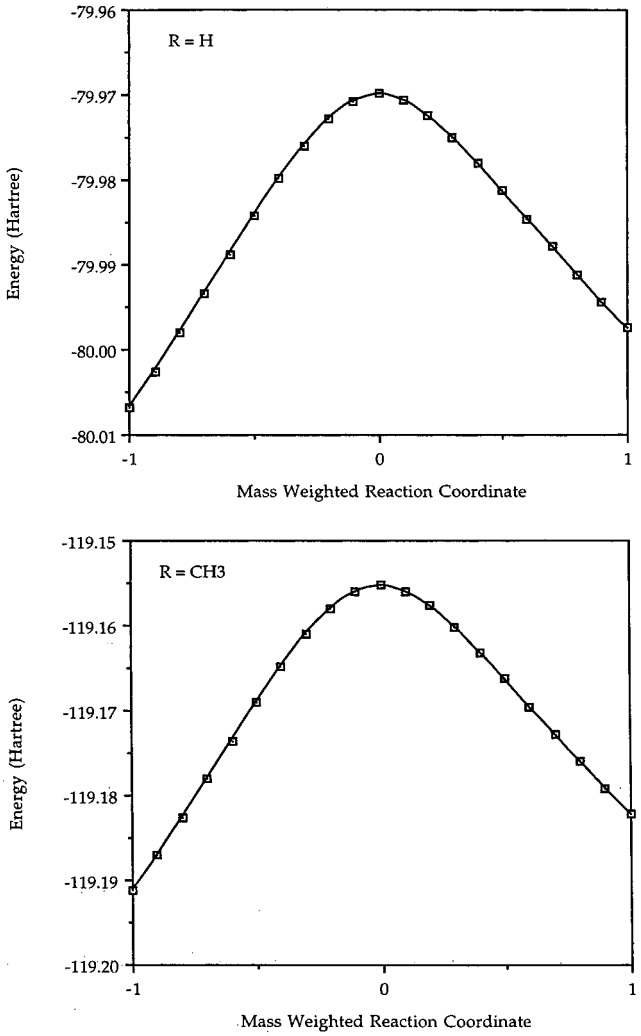

Figure 4. Energy of the reaction in Figure 2 plotted in intrinsic reaction coordinates.

Discussion

It is interesting to try to understand why the deviations from the Marcus equation exist. Marcus, Albey, and Murdoch provide several different derivations of the Marcus equation. However, the one that is the most relevant to the results in this paper is Chen and Murdoch's[23] derivation based on the bond additivity model. Recall that in the bond additivity model one calculates the $V(r_{CH}, r_{CC})$, the potential energy surface for reaction 8, from

$$V(r_{CH}, r_{CC}) = \Delta E_{CC}(\%CC) + \Delta E_{CH}(\%CH) + V_{Pauli}(r_{CH}, r_{CC}) \quad (12)$$

where r_{CH} and r_{CC} are the lengths of the C−H and C−C bonds; $\Delta E_{CC}(\%CC)$ is the change in $E_{CC}(\%CC)$, the energy of the C−C bond that breaks during the reaction; $\Delta E_{CH}(\%CH)$ is the change in $E_{CH}(\%CH)$, the energy of the C−H bond that forms during the reaction; %CH and %CC are the Pauling bond orders of

TABLE 4: Comparison of the Transition-State Positions Calculated by a Variety of Methods

R group	$\chi^{\ddagger}$ (Bockris)	$\chi^{\ddagger}$ (Marcus)	$\chi^{\ddagger}$ (Miller)	$\chi^{\ddagger}$ (Pauling)	$\chi^{\ddagger}$ (Geom)
H	0.59	0.46	0.42	0.54	0.54
CH_3	0.58	0.46	0.42	0.53	0.53
NH_2	0.55	0.44	0.38	0.51	0.51
CN	0.61	0.44	0.39	0.54	0.54
CF_3	0.59	0.47	0.44	0.54	0.54
C_6H_5		0.45	0.39	0.52	0.52

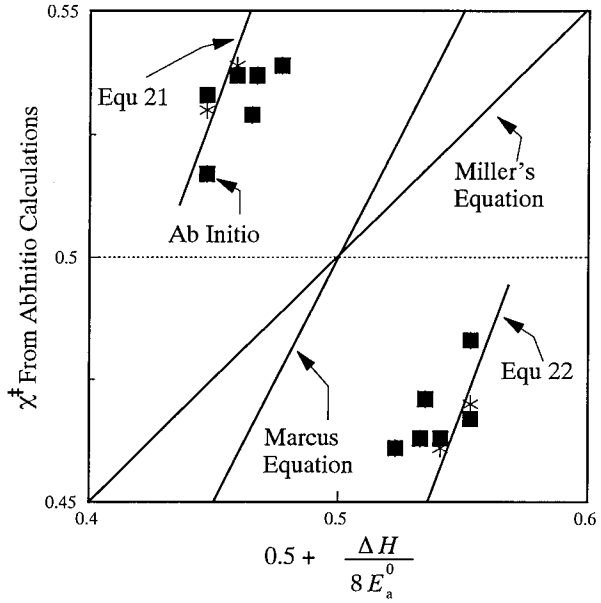

Figure 5. Comparison of the values of $\chi^{\ddagger}$ estimated from eq 3 with those estimated from the Marcus equation, eq 1, and the new model, eqs 21 and 22. The points are the ab initio calculations. The lines are the predictions of the various models.

the C−H and C−C bond, respectively; and $V_{\text{Pauli}}(r_{\text{CH}}, r_{\text{CC}})$ is the Pauli repulsion, which keeps the reactants apart. Chen and Murdoch[23] showed that if E_{CC} and E_{CH} are parabolic and if V_{Pauli} is small and constant, then the Marcus equation, eq 1, follows directly.

One can calculate E_{CC} and E_{CH} exactly from ab initio calculations for isolated methane and ethane molecules. $V(r_{\text{CH}}, r_{\text{CC}})$ is available from Figure 2. V_{Pauli} can then be calculated exactly from eq 12.

Figure 7 shows a plot of E_{CH} and E_{CC} as a function of the bond orders of the C−H and C−C bonds. The plots look as expected in both cases. The bond energy increases rapidly at small bond orders and then levels off at bond orders close to 1. Such a result is typical of what one would expect for a species that forms only a single bond.

What is surprising though is what happens when one plugs the numbers from Figure 7 into eq 12. Figure 8 shows a plot of the various terms in eq 11 for a reaction that follows the minimum energy reaction pathway for the reaction in Figure 2. Notice that in the initial part of the reaction the sum of E_{CC} and E_{CH} actually decreases as the reaction proceeds; that is, we get more energy back from forming the hydrogen−carbon bond than we lose in breaking the carbon−carbon bond. Note that according to Figure 6, it does not cost much energy to stretch the C−C bond slightly, and according to Figure 7, one gains considerable energy in forming a small fractional C−H bond. The result is that the first two terms in eq 11 produce a net attraction between the hydrogen and the ethane. In contrast, in the literature it is usually assumed that the sum of ΔE_{CC} and

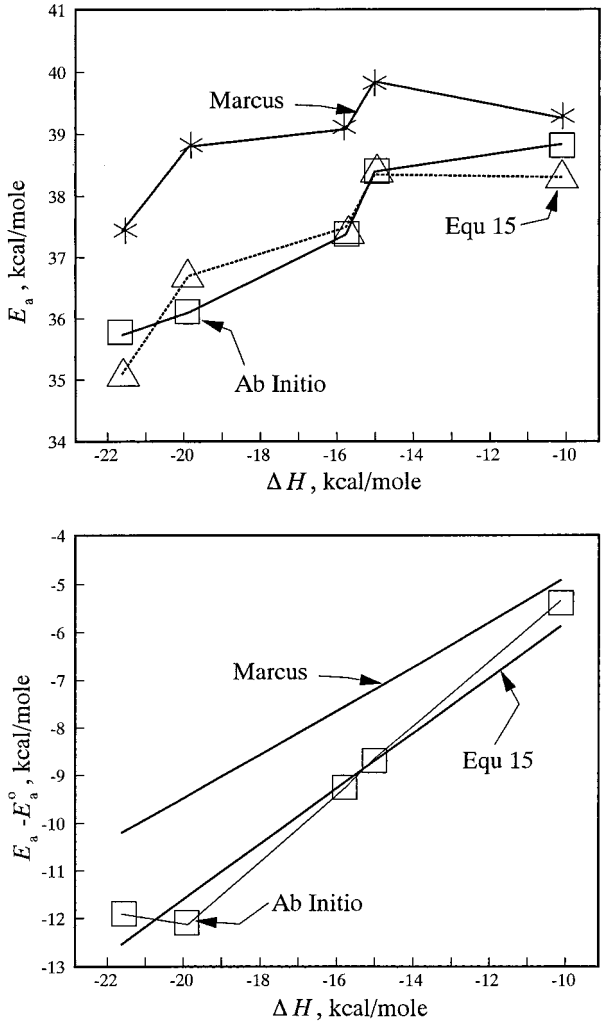

Figure 6. Plot of the activation barriers predicted by the Marcus equation and ab initio calculations as a function of the heat of reaction.

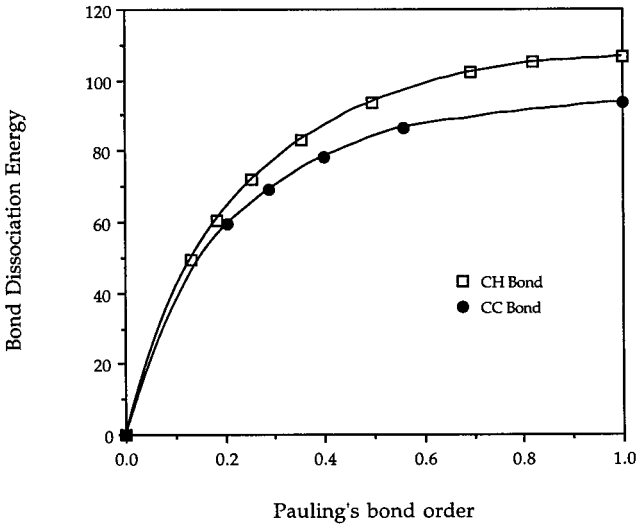

Figure 7. Plot of the energy of the C−C bond in ethane and the C−H bond in methane as a function of the Pauling bond order of the bond.

ΔE_{CH} produces a repulsive interaction and therefore a barrier to the reaction.

Our calculations show that in our case there is no barrier from ΔE_{CC} and ΔE_{CH}. Rather the main barrier arises from V_{Pauli}. In the previous literature people mention V_{Pauli} when they are

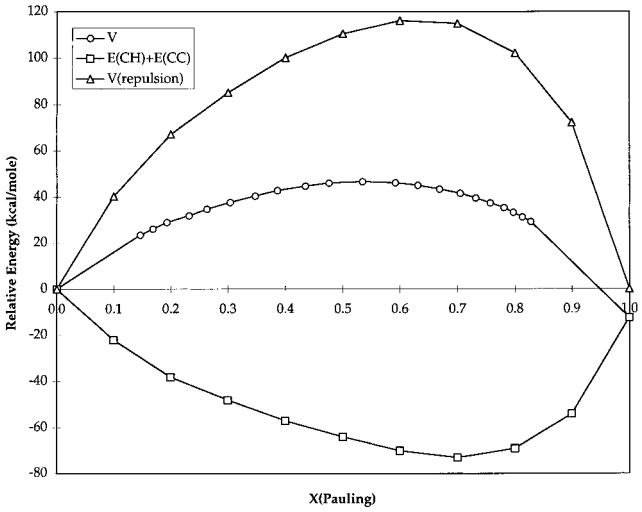

Figure 8. Plot of the various terms in eq 11 as the reaction proceeds.

discussing barriers to reaction, but usually assume that V_{Pauli} is small and Morse-like. However in our case, V_{Pauli} is huge.

Physically V_{Pauli} is associated with the rearrangement of the outer electrons before bonds begin to break. During reaction 9, an incoming hydrogen approaches an ethane along the C_{3v} axis of the ethane, as shown in Figure 3. When the reactants first come together, there is an electron−electron repulsion between the electron on the incoming hydrogen and the electrons on the hydrogen on the methyl group. That repulsion makes V_{Pauli} large.

It is interesting to look at a molecular orbital diagram to see how the Pauli repulsions arise. People usually do not present orbital diagrams in Hartree−Fock (HF) type calculations due to a uniqueness problem. If two occupied states have the same symmetry, then any sum of the two orbitals also satisfies the Shroedinger equation. As a result in general, one cannot define the orbitals uniquely in HF calculations. Nevertheless, one can create unique orbital diagrams, if one has a very symmetric system so that only a few states have the same symmetry, and then one uses core potentials and other tricks to get unique diagrams.

In our case, there were only three A_{1g} orbitals in the problem, and we could get a unique orbital diagram by maximizing the electron density in the bonds. More details on how one gets a unique diagram are given in Lee and Masel.[20]

Figure 9 shows a plot of the energies of the various MOs of hydrogen and ethane, calculated using a Mullikin state decomposition ignoring the core states. Ethane has D_{3d} symmetry. In ethane the $3A_{1g}$, $2A_{1g}$, $2A_{2g}$, $1E_u$, $3A_{1g}$, and $1E_g$ states are occupied, while the $3A_{2u}$ and higher are empty. Hydrogen has a single occupied 1s orbital and some empty 2s and 2p states.

When the hydrogen first approaches the ethane, the main interaction is between the 1s orbital in the hydrogen and the $3A_{1g}$ orbital in the ethane. There is a bonding state which we will label $3A_{1g}+1s$ and an antibonding state which we will label $3A_{1g}-1s$. Figure 9 shows the energy level we calculated for the $3A_{1g}+1s$ and the $3A_{1g}-1s$ states using the Mullikin state decomposition. The calculation was done for a case where the incoming hydrogen was still 2 Å away from the carbon. In this case the $3A_{1g}+1s$ bonding level of the system has only been stabilized by 0.02 hartrees. One does not want to overinterpret these changes due to the well-known uniqueness problem mentioned above. Still there is a 28 kcal/mol repulsive interaction, which is surprising at such a small reaction coordinate.

Figure 10 shows how the $3A_{1g}-1s$ state changes during the reaction. The 1s state starts out spherical, while the $3A_{1g}$ state starts out with C_{3v} symmetry. There is a completely symmetric center lobe and two outer lobes. The outer lobes actually have 3-fold symmetry, but if you view them in cross section along the plane of one of the C−H bonds, the outer lobes look kidney shaped, with more electron density along the C−H bond in the plane of the paper than between the C−H bonds above and below the paper.

Now when the reaction proceeds, the $3A_{1g}$ and 1s orbitals significantly distort. The left lobe in the $3A_{1g}$ orbital shrinks, while the hydrogen 1s orbital changes shape significantly. Notice that much of the orbital distortion occurs at small Pauling bond orders. For example, Figure 9b is a case where the incoming hydrogen atom is 2 Å away from the carbon. When the C−H is 2 Å away from the carbon, the C−H bond has a Pauling bond order of only 0.05, while the carbon−carbon in the ethane still has a bond order of 0.95. However, the 1s orbital in the hydrogen and the leftmost lobe of the $3A_{1g}$ orbital on the ethane have distorted significantly. Energetically, there is a net repulsion of almost 30 kcal/mol. Interestingly, the center lobe of the $3A_{1g}$ orbital (i.e., the carbon−carbon bond) has hardly changed. Physically the electron in the incoming hydrogen atom repels the electrons in the CH_3 group. This produces a significant Pauli repulsion even before the carbon−carbon bond scission begins.

Similarly, at the end of the reaction, there is a Pauli repulsion between the reactants that occurs after all of the bonds in the system have reached their equilibrium bond lengths. Figure 10 shows an orbital interaction diagram for that case. A planar methyl radical has electrons in the $2A_1$, $1E'$, and $1A_2''$ states, while the methane has electrons in the $2A_1$ and $1T_2$ states. The $1T_2$ states split into an A_2 state and two E states in C_{3V} symmetry. When the methyl radical reacts with the methane, the $2A_1$ state in the methyl radical reacts with the $2A_1$ state in the methane to produce a bonding and antibonding pair with energies similar to those one would expect. Similarly the E states on the methyl interact with the E states on the methane to form a bonding and antibonding pair. The A_2 states on the methyl group and that on the methane also interact to form a bonding and antibonding pair. However, when we calculate the energies for a situation where there is a very long carbon−carbon bond, the bonding (A_2+T_1) state lies well above the T_1 state in methane. The result is a substantial Pauli repulsion.

Figure 10g shows an orbital diagram for that case. Notice that the molecular orbitals in the methyl group and methane are significantly distorted, yet the electron density between the carbon and the hydrogen has hardly changed, and there is no evidence for a bonding interaction between the carbons. In this example, the Pauling bond order for the C−H is still 0.98 and the Pauling bond order for the carbon−carbon is only 0.1. Physically the electrons on the methyl are being repelled by the electrons on the hydrogens in the methane; this produces a large orbital distortion before bond scission begins.

There is another interesting detail in Figure 10. Focus for the moment on the center lobe on the $3A_{1g}$ state on ethane. Notice how the center lobe distorts. The lobe starts out symmetric and provides a continuous bond between the two carbon atoms in the ethane. The lobe distorts, but even at $\chi = 0.3$, the lobe bridges between the two carbons, implying that there is still an intact carbon−carbon bond. However, there is an important change between $\chi = 0.31$ and $\chi = 0.73$. At $\chi = 0.73$ the lobe no longer extends from one carbon to the next. Rather, there is a node between the two carbons, which implies

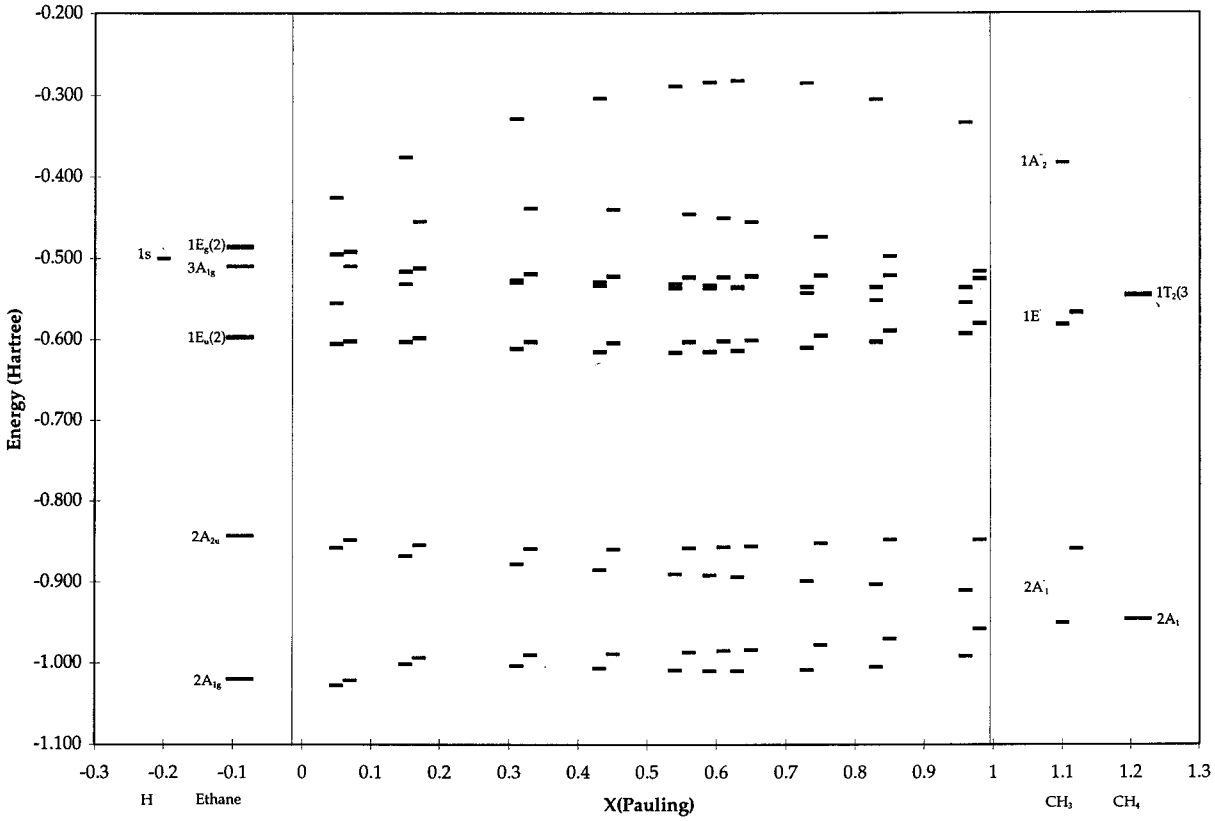

Figure 9. Plot of the change in the orbital energies as the reaction proceeds calculated with the Mullikin orbital decomposition.

that there is an antibonding interaction between the two carbons. That antibonding interaction grows as the reaction proceeds. Similarly, the hydrogen−hydrogen bond is antibonding at the reactants and then switches to being bonding at the products. Figure 11 shows a blow up of the transition between "reactant-like" and "product-like" molecular orbitals. Interestingly, the switch in the character of the C−H and C−C bonds occurs at $\chi = 0.56$ (i.e., a point later than the transition state).

Now it is interesting to compare these results to the predictions of the Marcus model and Miller's results. Recall that Murdochs' and Albey's extension of the Marcus equation to atom-transfer reactions assumes that the reaction starts going up a "reactant-like" curve and then switches at a curve crossing and goes down a "product-like" curve as indicated in Figure 1. Our results in Figure 10 show that the MOs start out "reactant-like," with an intact C−C bond. However, during the course of the reaction the MOs switch to "product-like" MOs with an intact C−H bond. Interestingly, the transition state (i.e., the saddle point on the potential energy surface) does not correspond to the curve crossing. Rather the saddle point on the potential energy surface occurs at $\chi = 0.547$, while the curve crossing occurs at $\chi = 0.56$.

The other key piece of physics, which is ignored when one tries to extend the Marcus model to atom-transfer reaction, is that there are big orbital distortions before the reaction begins. Recall that at $\chi = 0.05$ the energy of the system has gone up by 28 kcal/mol. Yet Figure 10b shows that the carbon−carbon is largely intact. Figure 8 suggests that the bond distortions are producing a barrier of more than 50 kcal/mol. This barrier is ignored in the Murdoch extension of the Marcus equation to atom- and ligand-transfer reactions. Consequently, Marcus' equation does not correctly predict either the energy or the value of χ at the transition state for ligand-transfer reactions.

Another way to look at this result is that the basic assumption in extending the Marcus equation to atom-transfer reactions, i.e. that the energy looks parabolic in the reaction coordinate, does not work for atom- or ligand-transfer reactions. When one assumes that the system follows a parabolic potential in χ, one is in effect assuming that there are only small variations in the energy of the system until one starts to stretch the various bonds, i.e. $dE/d\chi = 0$ at the reactants and products, and $dE/d\chi$ grows as one stretches the bonds. This might be true for a simple electron-transfer reaction. However, in the cases considered in this paper, $dE/d\chi$ is large near the reactants and products and decreases moving toward the transition state. This is exactly the opposite of what the Marcus equation assumes. Consequently, the Marcus equation does a poor job in predicting the position state for atom-transfer reactions.

Now, while that is probably a surprising result to many people, perhaps it should not be. After all, Marcus[2] showed that eq 1 would not be expected to work for atom-transfer reactions. People use eq 1 anyway, but it is not surprising that it does not work considering that Marcus' derivation is not appropriate for atom-transfer reactions.

A New Model

One can derive a formulation that works based on Polayni and co-workers[24] extension of the London−Eyring−Pauling potential. According to Polayni and co-workers, one can approximate $V(r_{CH}, r_{CC})$, the potential energy surface for a ligand-transfer reaction, as the sum of the Morse potential plus a repulsive term due to the Pauli repulsions, i.e.

$$V(r_{CH}, r_{CC}) = w_{CH}\{\exp(\alpha_1(r_{CH,equ} - r_{CH})) - 1\}^2 - w_{CH} + w_{CC}\{\exp(\alpha_2 (r_{CC,equ} - r_{CC})) - 1\}^2 - w_{CC} + V_{Pauli} \quad (13)$$

where w_{CH} and w_{CC} are the bond energies of the C−H and C−C bonds, r_{CH} and r_{CC} are the lengths of the C−H and C−C bonds, $r_{CC,equ}$ and $r_{CH,equ}$ are the equilibrium bond lengths, α_1 and α_2

are constants, and V_{Pauli} is the strength of the Pauli repulsion. For the derivation here it is useful to approximate the Pauli repulsion as a simple exponential:

$$V_{\text{Pauli}} = V_0 \exp(-\alpha_3 r_{\text{CH}} - \alpha_4 r_{\text{CC}}) \tag{14}$$

where V_0, α_3, and α_4 are constants. Combining eqs 13 and 14 and substituting the Pauling bond order for the C−H and C−C bonds into the equation yields

$$V(r_{\text{CH}}, r_{\text{CC}}) = w_{\text{CH}}((n_{\text{CH}})^{p_{\text{CH}}} - 1)^2 + w_{\text{CC}}((n_{\text{CC}})^{p_{\text{CH}}} - 1)^2 - w_{\text{CH}} - w_{\text{CC}} + V_{\text{p}}(n_{\text{CH}})^{p_{\text{CH}}q_{\text{CH}}}(n_{\text{CC}})^{p_{\text{CH}}q_{\text{CH}}} \tag{15}$$

where n_{CH} and n_{CC} are the Pauling bond order for the C−H and C−C bonds and

$$\begin{aligned} p_{\text{CH}} &= \alpha_1 a \\ p_{\text{CH}} &= \alpha_2 a \\ q_{\text{CH}} &= \frac{\alpha_3}{\alpha_1} \\ q_{\text{CH}} &= \frac{\alpha_4}{\alpha_2} \\ V_{\text{p}} &= V_0 \exp(\alpha_3 r_{\text{CH,equ}} + \alpha_4 r_{\text{CC,equ}}) \end{aligned} \tag{16}$$

In our example p_{CC} and p_{CH} are approximately 1.0, while q_{CC} and q_{CH} are less than 1; that is the Pauli repulsion starts before bond formation.

Figure 12 shows a plot of the potential energy surface calculated from eq 15. Figure 12 looks quantitatively similar to the potential energy surface in Figure 2, which suggests that the approximation in eq 15 does a reasonable job of fitting the potential energy surface.

Equation 15 also does a reasonable job of fitting the results in Figure 7. In particular the sum of the first two terms in eq 15 decreases as the reaction proceeds. The actual bond energy decreases. There is a barrier only because of the last term in eq 15, i.e. the Pauli repulsion.

One can derive an equation for $n^{\ddagger}_{\text{CH}}$ and $n^{\ddagger}_{\text{CC}}$, the bond order at the saddle point in Figure 11, by setting $\mathrm{d}V/\mathrm{d}n = 0$ and solving, the result is

$$(n^{\ddagger}_{\text{CC}})^{p_{\text{CC}}} = \frac{D_{\text{CC}} - 1}{D_{\text{CC}}D_{\text{CH}} - 1} \tag{17}$$

$$(n^{\ddagger}_{\text{CH}})^{p_{\text{CH}}} = \frac{D_{\text{CH}} - 1}{D_{\text{CC}}D_{\text{CH}} - 1} \tag{18}$$

with

$$D_{\text{CC}} = \frac{q_{\text{CC}}V_{\text{p}}}{2w_{\text{CC}}} n_{\text{CC}}^{p_{\text{CC}}(q_{\text{CC}}-1)} n_{\text{CH}}^{p_{\text{CH}}(q_{\text{CH}}-1)} \tag{19}$$

$$D_{\text{CH}} = \frac{q_{\text{CH}}V_{\text{p}}}{2w_{\text{CH}}} n_{\text{CC}}^{p_{\text{CC}}(q_{\text{CC}}-1)} n_{\text{CH}}^{p_{\text{CH}}(q_{\text{CH}}-1)} \tag{20}$$

If $p_{\text{CC}} = p_{\text{CH}} = 1$, the position of the transition state becomes

$$\chi^{\ddagger}_{\text{F}} = \frac{n^{\ddagger}_{\text{CH}}}{n^{\ddagger}_{\text{CC}} + n^{\ddagger}_{\text{CH}}} = \frac{(D_{\text{CH}} - 1)}{D_{\text{CH}} + D_{\text{CC}} - 2} \tag{21}$$

Similarly the position of the transition state for the reverse reaction becomes

$$\chi^{\ddagger}_{\text{F}} = \frac{n^{\ddagger}_{\text{CC}}}{n^{\ddagger}_{\text{CC}} + n^{\ddagger}_{\text{CH}}} = \frac{(D_{\text{CC}} - 1)}{D_{\text{CH}} + D_{\text{CC}} - 2} \tag{22}$$

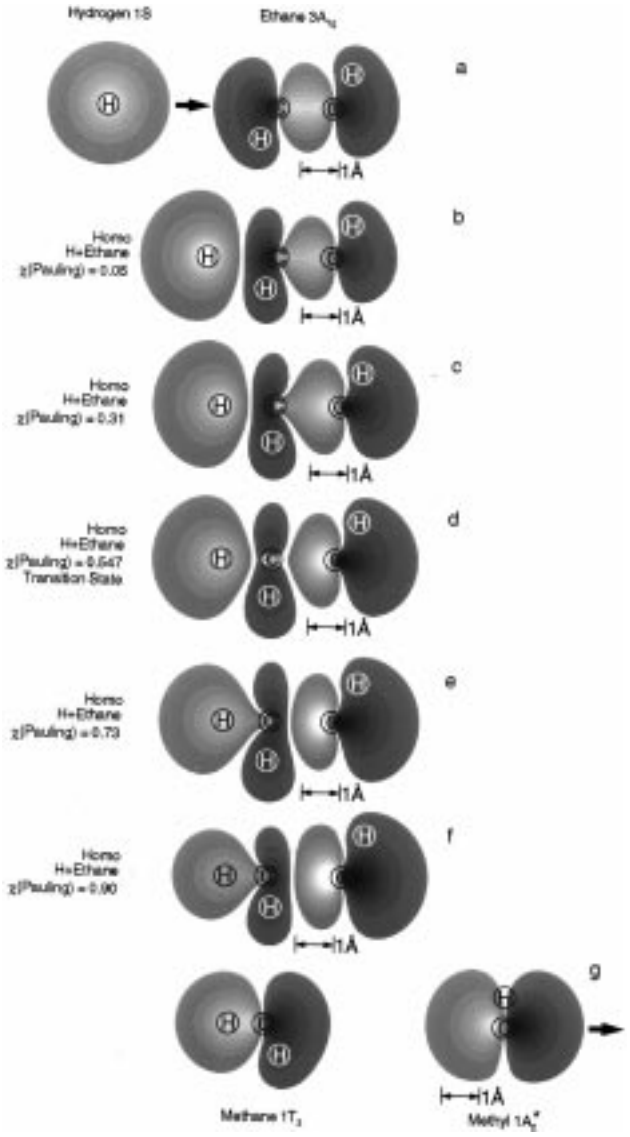

Figure 10. Changes in the $3A_{1g}$−1s orbital as the reaction proceeds calculated as described in the text.

Figure 13 compares $\chi^{\ddagger}$ calculated from the Marcus equation, eq 1, to $\chi^{\ddagger}$ calculated from eqs 21 and 22. Notice that when $q_{\text{CC}} = q_{\text{CH}} = 1.0$, the behavior looks quite like that predicted by the Marcus equation. In particular $\chi^{\ddagger}$ shifts monotonically as ΔH_{r} changes. The slope is slightly different than predicted from the Marcus equation, but the differences are small.

However, when $q_{\text{CC}} = 0.77$, the results change. The Pauli repulsions shift the transition state toward the methane product. There is a subtlety created by the definition of $\chi^{\ddagger}$. Notice, that if we run the forward reaction

$$\text{H} + \text{CH}_3\text{R} \rightarrow \text{HCH}_3 + \text{R}$$

the transition state shifts toward the methane. Methane is the product so $\chi^{\ddagger}$ is increased. However, if we consider the reverse reaction

$$\text{HCH}_3 + \text{R} \rightarrow \text{H} + \text{CH}_3\text{R} \tag{23}$$

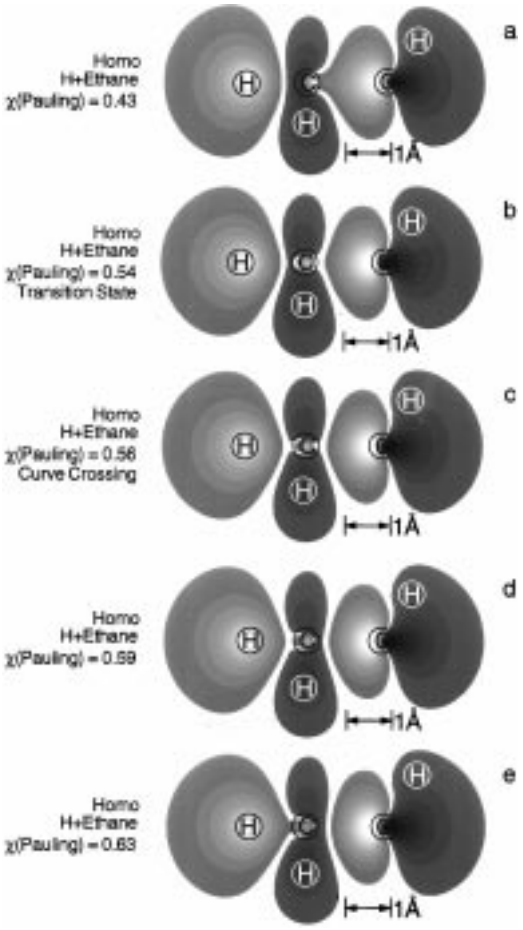

Figure 11. Series of orbital diagrams near the curve crossing in Figure 10. The light colored orbitals are positive lobes, and the dark colored orbitals are negative lobes.

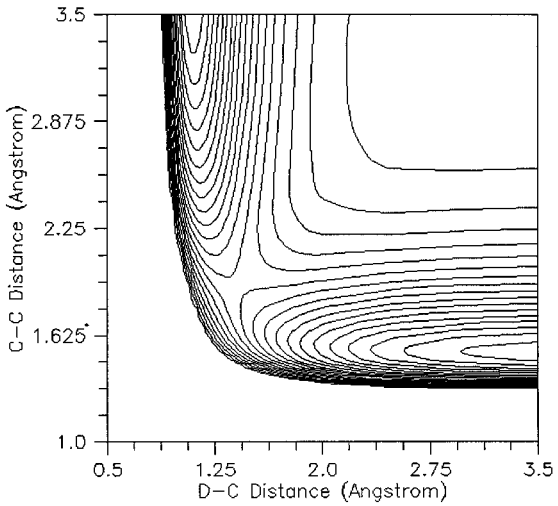

Figure 12. Plot of the potential in eq 15, $p_{CH} = 1$, $p_{CC} = 1$, $q_{CH} = 1$, $q_{CC} = 0.77$, $w_{CC} = 89$ kcal/mol, $w_{CH} = 104$ kcal/mol, $V_p = 400$ kcal/mol.

we still shift the transition state toward methane. In this case methane is the reactant, so by definition $\chi^{\ddagger}$ is decreased. In a more general way $\chi^{\ddagger}$ is not a unique function of $\Delta H/E_A^{\circ}$. Instead $\chi^{\ddagger}$ changes according to whether we are considering the forward or reverse reaction.

Interestingly, we observe the same things in our ab initio calculations. Figure 5 compares the position of the transition state calculated from eqs 21 and 22 to those from the ab initio calculations. Notice that the ab initio results fall into two

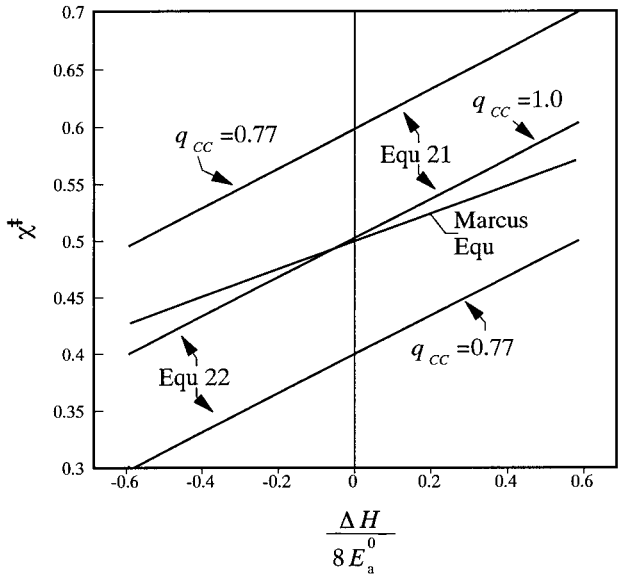

Figure 13. Comparison of $\chi^{\ddagger}$ calculated from the Marcus equation with $\chi^{\ddagger}$ calculated for eqs 21 and 22: (a) $q_{CC} = 1.0$, (b) $q_{CC} = 0.77$, $p_{CC} = p_{CH} = q_{CH} = 1.0$.

clusters, just as we expect from eqs 21 and 22. Equations 21 and 22 fit the ab initio calculations much better than the Marcus equation. Clearly, then, one can get a reasonable fit from the data including the Pauli repulsions into the model.

Conclusions

In summary then, we find that the Marcus equation does not do a good job of predicting the position of the transition state for ligand-transfer reactions. The Marcus equation considers the energies associated with the formation and destruction of bonds, but not the Pauli repulsion, which occurs before bond formation begins. In the reactions considered here, the Pauli repulsions of these bonds play a dominant role. We also showed that if one explicitly considers the Pauli repulsions, one can derive an equation that fits the data. The conclusion from our study is that Pauli repulsions are quite important in atom- and ligand-transfer reactions and so one must consider them to get a suitable model.

Acknowledgment. This work was supported by the National Science Foundation under Grant CTS 96-10115. The authors would like to thank Rudy Marcus for helpful discussions.

References and Notes

(1) Marcus, R. A. *J. Phys. Chem.* **1968**, *72*, 891.
(2) Marcus, R. A. *J. Am. Chem. Soc.* **1969**, *91*, 7224.
(3) Lee, W. T.; Masel, R. I. *J. Phys. Chem.* **1966**, *100*, 10945.
(4) Yamataka, H.; Nagase, S. *J. Org. Chem.* **1988**, *53*, 3232.
(5) Shaik, S. S.; Schlegel, H. B.; Wolfe, S. *Theoretical Aspects of Physical Organic Chemistry: The S_N2 Mechanism*; John Wiley and Sons, Inc.: New York, 1992.
(6) Pross, A.; Shaik, S. S. *New J. Chem.* **1988**, *13*, 427.
(7) Pauling, L. *J. Am. Chem. Soc.* **1947**, *69*, 542.
(8) Hammond, G. S. *J. Am. Chem. Soc.* **1955**, *77*, 334.
(9) Brønsted, J. N. *Chem. Rev.* **1928**, *5*, 231.
(10) Leffler, J. E. *Science* **1953**, *117*, 340.
(11) Bockris, J. O. M. *Modern Electrochemistry*; Plenum: New York 1970; Vol. 2, p 1110.
(12) Miller, A. R. *J. Am. Chem. Soc.* **1978**, *100*, 1984.
(13) Agmon, N. *J. Chem. Soc., Faraday Trans. 2* **1978**, *74*, 388.
(14) Schlegel, H. B. *J. Phys. Chem.* **1988**, *92*, 3075.
(15) Curtiss, L. A.; Raghavachav, K.; Trucks, G. W.; Pople, J. A. *J. Chem. Phys.* **1991**, *94*.
(16) Gonzalez, C.; Schlegel, H. B. *J. Phys. Chem.* **1990**, *94*, 5523.
(17) Frish, M. J.; Trucks, G. W.; Schlegel, H. B.; Gill, P. M. W.; Johnson, B. G.; Wong, M. W.; Foresman, J. B.; Robb, M. A.; Head-Gordon, M.; Replogle, E. S.; Comperts, R.; Andres, J. L.; Raghavachari, K.; Binkley, J. S.; Gonzalez, C.; Martin, R. L.; Fox, D. J.; Defrees, D. J.; Baker, J.;

Stewart, J. J. P.; Pople, J. A. *Gaussian 92/DFT*, Revision G.2; Gaussian, Inc.: Pittsburgh, PA, 1993.

(18) Frish, M. J.; Trucks, G. W.; Schlegel, H. B.; Gill, P. M. W.; Johnson, B. G.; Robb, M. A.; Cheeseman, J. R.; Keith, T.; Peterson, G. A.; Montgomery, J. A.; Raghavachari, K.; Al-Laham, M. A.; Zakrzewski, V. G.; Ortiz, J. V.; Foresman, J. B.; Peng, C. Y.; Ayala, P. Y.; Chen, W.; Wong, M. W.; Andres, J. L.; Replogle, E. S.; Gomperts, R.; Martin, R. L.; Fox, D. J.; Binkley, J. S.; Defrees, D. J.; Baker, J.; Stewart, J. J. P.; Head-Gordon, M.; Gonzales, C.; Pople, J. A. *Gaussian 94*, Revision B.3; Gaussian, Inc.: Pittsburgh, PA, 1995.

(19) *CRC Handbook of Chemistry and Physics*, Lide, D. R., Ed.; CRC Press: Boca Raton, 1992−1993.

(20) Lee, W. T.; Masel, R. I. Submitted.

(21) Chen, M.; Murdoch, J. R. *J. Am. Chem. Soc.* **1984**, *106*, 4735.

(22) Haim, A; Sutin, N. *J. Appl. Chem. Biotechnol.* **1966**, *88*, 434.

(23) Albey, W. J. *Annu. Rev. Phys. Chem.* **1980**, *31*, 227.

(24) Kuntz, J.; Nemeth, E. M.; Polanyi, J. C.; Rosner, S. D.; Young, C. E. *J. Chem. Phys.* **1966**, *44*, 1168.

(25) Polayni, J. C.; Wong, W. H. *J. Chem. Phys.* **1969**, *51*, 1439.